Chaotic Mixing in a Free Helix Extruder using a New Solution to the Biharmonic Equation

Gregory A. Campbell[†], Ross Taylor[*], Mark D. Wetzel[***,]

Shaji Chempath, Sirisha Bomma, Samuel St. John, Diana Hunt, David L. Powers[**],

[*]Department of Chemical and Biomolecular Engineering

[**]Department of Mathematics and Computer Science

[†]Emeritus Chemical Engineering Professor

Clarkson University

Potsdam, NY 13699. U.S.A.

[***]Florence, Oregon

Abstract

A recently published approach for modeling the cross flow in an extruder channel using a new solution to the biharmonic equation is utilized in a study of chaotic mixing in a free helix single screw extruder. This novel extruder was designed and constructed with the screw flight, also referred to as the helix, detached from the screw core. The flight-helix had straight sides that more closely emulated rectangular channel theory than the nominal sloped sides of a conventional single screw channel. Each of the screw elements could be rotated independently to obtain chaotic motion in the screw channel. Using the new extruder, experimental evidence for the increased mixing of a dye, for both a Dirac and droplet input, with a chaotic flow field relative to the traditional residence time distribution is presented. These experimental results are compared using the new biharmonic equation-based model. Comparing the experimental chaotic mixing with theoretical calculations was facilitated by a recently published technique for accurately placing the

dye in the extruder channel. Because of the ability to periodically rotate only the flight/helix, the chaotic mixing results are minimally confounded by the existence of Moffatt eddies.

Keywords:

Single screw extruder, Cross channel flow, Biharmonic equation, Residence Time, Chaotic Mixing

Introduction

The field of polymer-processing is dominated with the conversion of polymers into useful products. The single screw extruder, in which a screw rotates in a cylindrical barrel, is the central component of an entire class of polymer processing machinery. A conventional screw is made up of a core and a flight-helix that is machined such that it is permanently attached to the screw core. Most polymers pass through a single screw extruder at least once in their production path, starting from the polymerization reactor through to the final form of the product. An important use of the single screw extruders is to add small quantities of highly filled pellets to the base resin for both color concentrates or stabilizing additives to polymer resins.

The first known analysis of the extruder screw pump came early in the twentieth century[1,2] and it was the first "complete" down channel "drag flow" analysis on a screw pump. Substantial developments have since taken place, both for optimizing the mechanical design and engineering analysis of the fluid flow section of the extrusion process. These early fluid mechanical developments have been extended to the different sections of the extruder, including solids conveying, melting and melt flow. Extensive reviews of the development in our understanding of single screw extruders may be found elsewhere[3,4]. The single screw extruder is not a very effective mixer, and many mechanical structures have been invented and machined into the screw to improve mixing[5]. The screw section responsible for mixing was typically characterized by its closeness to the outer barrel to generate the high shear stress required for a dispersive mixing (e.g.,

Maddock section and blister ring), or by a large number of small units affixed to the root of the screw for a distributive mixing (e.g., pin and pineapple mixing sections) including the Saxon mixer (see Chapter 8 of Ref. [4]). The poor mixing in single screw pumps and extruders is characterized by the well-known long-tailed residence time. This is caused by the effectively rectangular screw channel shape that produces a secondary flow in the corners with a very small down channel velocity; the Moffat eddy as shown in Figure 1. This secondary flow is a major cause of the poor mixing in single screw pumps[4,12].

As detailed later in this paper, there have been many efforts to use chaotic mixing in single screw extruder. All the results from these developments were confounded because they used modifications of traditionally designed screws which produced Moffat eddies. This paper will focus on chaotic mixing experiments carried out in a novel "free helix" extruder that had the flight-helix as a separate element of the extruder screw which was operated to produce deterministic chaotic mixing. A new technique was developed to introduce the tracer that better correlates with the predictions of a recently published three-dimensional (3-D) model based on a solution of the biharmonic equation to simulate the flow of Newtonian viscous fluids in the extruder[6]. The device used in this research had what is referred to as a deep channel with an aspect ratio $H/W = 0.85$. The modeling of single screw extruder flow is next reviewed to set the foundations of the chaotic mixing analysis.

The flow field in a single-screw extruder channel has been traditionally modeled by unwrapping the screw channel and then approximating the flow induced in a rectangular channel with one of the walls (top) moving and with the modeling focused on the down channel drag flow. In some textbooks, it has been suggested that for this flow analysis one can throw away the flight-

helix; that is, restrict the analysis to a one-dimensional down channel flow. The resulting design equation is:

$$Q_{flow} = \tfrac{1}{2} WHV_{bz} \tag{1}$$

where Q_{flow} is the volumetric flow rate, W is the rectangular channel width, H is the channel height and V_{bz} is the down channel velocity.

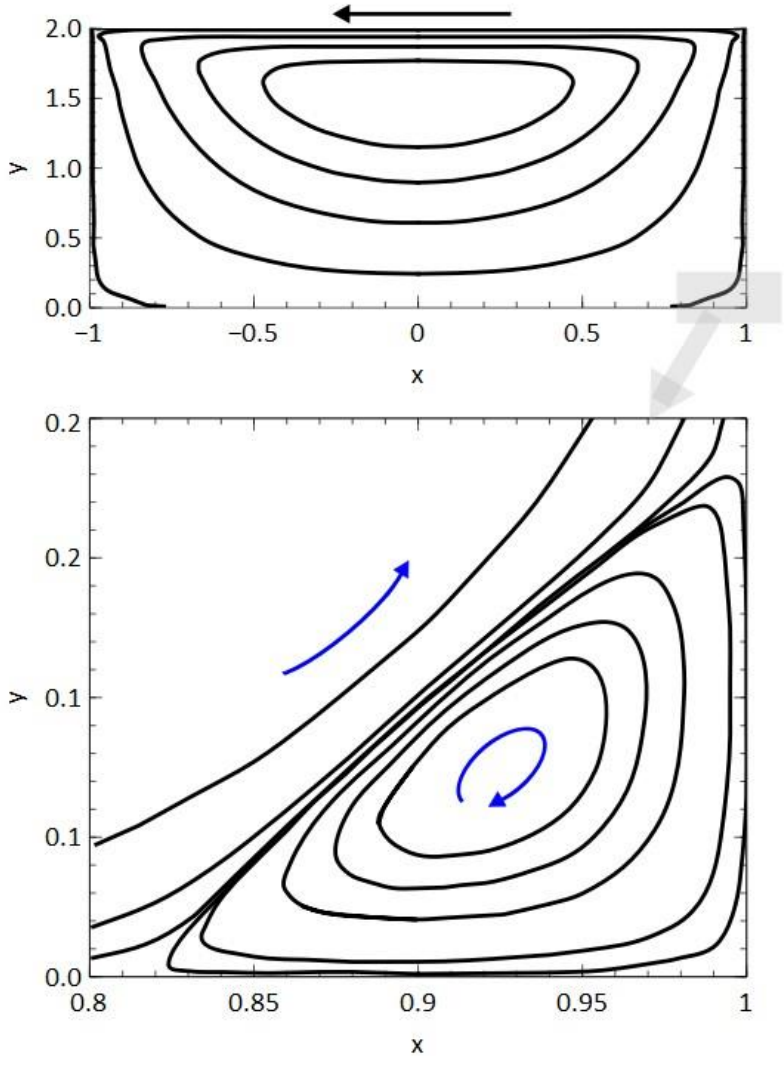

Figure 1. Streamlines in fluid in a screw extruder with aspect ratio of 2 and the top wall moving from right to left. Top: Large scale motion. Bottom: Expanded view of Moffat eddy that forms in the lower right corner. A similar eddy will form in the bottom left corner.

These models are based on a change in the process physics that involves moving the barrel instead of moving the screw[1,2,3,7,8]. This approach is often referred to as the shallow channel approximation because it is only accurate as *H* approaches 0 and has traditionally been use for channels with depths less than 10% of the screw diameter. This assumption requires that the *z*-direction screw core based shear rate must be maintained when the barrel is moved, thus the barrel must be slowed as the channel depth in increased. In the limit, this leads to a prediction of decreased flow rate as the channel gets deeper. This is the opposite of what was found experimentally[4]. In Figure 2, the screw core, flight-helix, and the barrel are different colors to indicate that they are independent elements in the new extruder. In the analysis developed in this paper, the core and the flight-helix can be rotated independently. The variables are transformed from the Eulerian to the Lagrangian frame to remove the complexities of a moving boundary problem. These transformations are demonstrated in Figure 2. When the observer remains at the laboratory coordinate system, the reference frame transformation results in the *barrel rotation frame*. With this frame change, the process physics is altered by stopping the screw and moving the barrel. This comes with the well-known limitation of the shallow channel restriction discussed above. Campbell et al.[9,10] showed experimentally that this is not the case, and they developed an analysis that predicts that as the screw core diameter decreases the flow rate continues to increase.

The Campbell et al.[9,10] analyses are based on the transformation advocated by Melvern[11] who points out that the appropriate manner to change the reference frame is to change the position of the observer and not to change the process physics. In this case, the observer is moved from the laboratory coordinates to a location in a coordinate system attached to the flight. In this *transformed (moving) reference frame* shown in Figure 2, the observer is standing on the yellow

coordinate system (but difficult to see due to his/her smaller size). In this *transformed (moving) reference frame*, the flow rate is given by (see Chapter 7 in Ref. [4]):

$$Q_{flow} = \frac{W}{\sin(q)} \int_0^H \left[\begin{array}{l} \left(V_{sx} \left(1 + \frac{H}{Rc} \right) \frac{y}{H} \left(2 - 3\frac{y}{H} \right) + V_{sx} \left(1 + \frac{y}{Rc} \right) \right) \cos(q) \\ + \left(\frac{y}{H} V_{sz} \left(1 + \frac{H}{Rc} \right) - V_{sz} \left(1 + \frac{y}{Rc} \right) \right) \sin(q) \end{array} \right] dy \qquad (2)$$

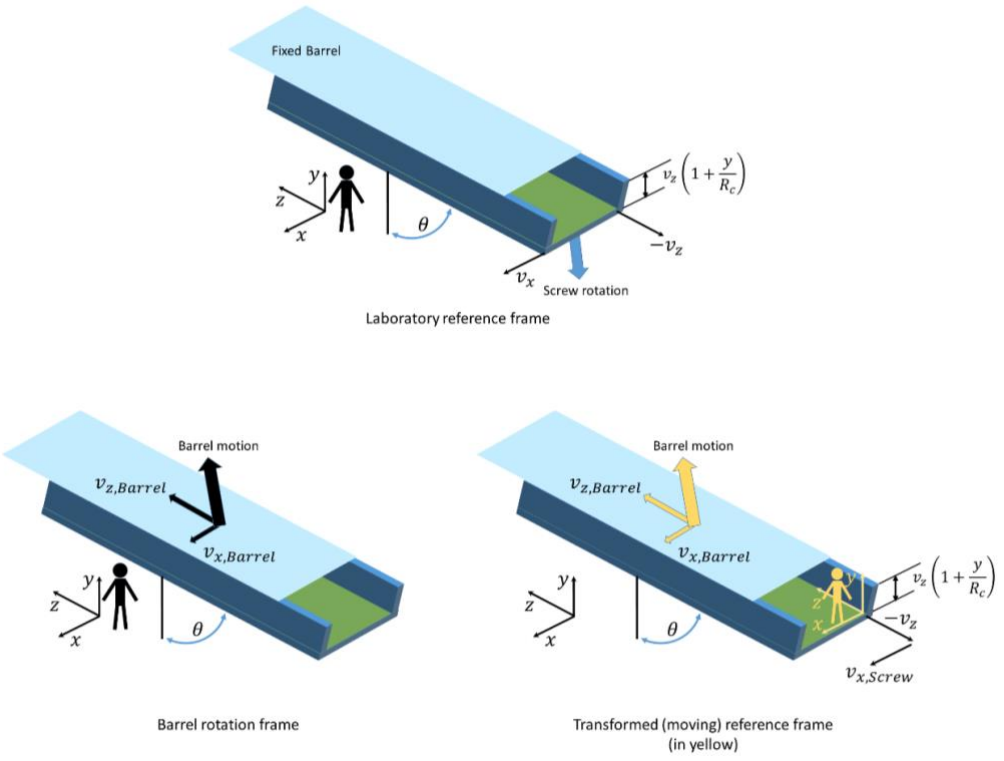

Figure 2. Reference Frame Transformation.

It is apparent from Eq. 2 that the pump is the flight-helix when the screw is rotated and that the core drag flow drags fluid back toward the screw entrance. Campbell and Spalding[4] have shown that by integrating and collecting terms, one develops the same form of the flow design equation, Eq. 1, from Eq. 2. Since the dominant flow is caused by the flight-helix, the barrel

velocity, V_{bz}, does not decrease as the core diameter decreases. This would be the expected result since velocity is frame indifferent. A recent numerical analysis of screw channel flow and Moffat eddies found that by keeping the barrel interface velocity independent of the channel depth, the results were consistent with those found using Eq. 2[12]. These transformed (moving) reference frame concepts are utilized in the following development: the boundary conditions at the barrel of the flight-helix, V_b, which is the velocity of the flight-helix next to the barrel.

Single-screw extruders used in the plastics industry typically convert the feedstock of plastic pellets into a molten polymer generally at high pressure to be extruded through a die. Stokes flow of molten liquid in the extruder channel is essentially considered a valid assumption. Many proposed modifications were made in rectangular channels, stirred tank reactors and extruders to achieve better mixing, often relying on the development of chaotic structures in the flowing fluids[13-17]. The flow field in a single-screw extruder channel was approximated as the flow induced in a rectangular channel with one of the walls (top wall) moving as published by Middleman[7], and Chella and Ottino[8]. Ottino, Rising, and Chien[14] published one of the typical cross-channel flow patterns representing particle trajectories that were computationally obtained over the entire cross section of the extruder channel. This fluid motion limits the effectiveness of the mixing because the fluid elements can only be stretched in the cross and down channel directions.

Chaotic Mixing

To introduce deterministic chaos, a new version of the extruder pumping section was designed with a clear glass barrel that allowed the screw core and the screw helix to rotate independently[15]. Wiggins and Ottino published a review that introduces the fundamentals and

many applications of chaotic mixing[16]. The glass barrel facilitated observing the mixing mechanism as well as allowing video analysis, per Figure 3. The new laboratory extruder was different from normal single-screw extruders, because the helix-flight of the screw was detached from the core of the screw and they both could be moved independently. Thus, the fluid can undergo laminar chaotic flow due to an added degree of freedom such as having the fluid elements produce the "baker's fold." Visualization experiments were also conducted in this laboratory free helix extruder with a glass barrel.

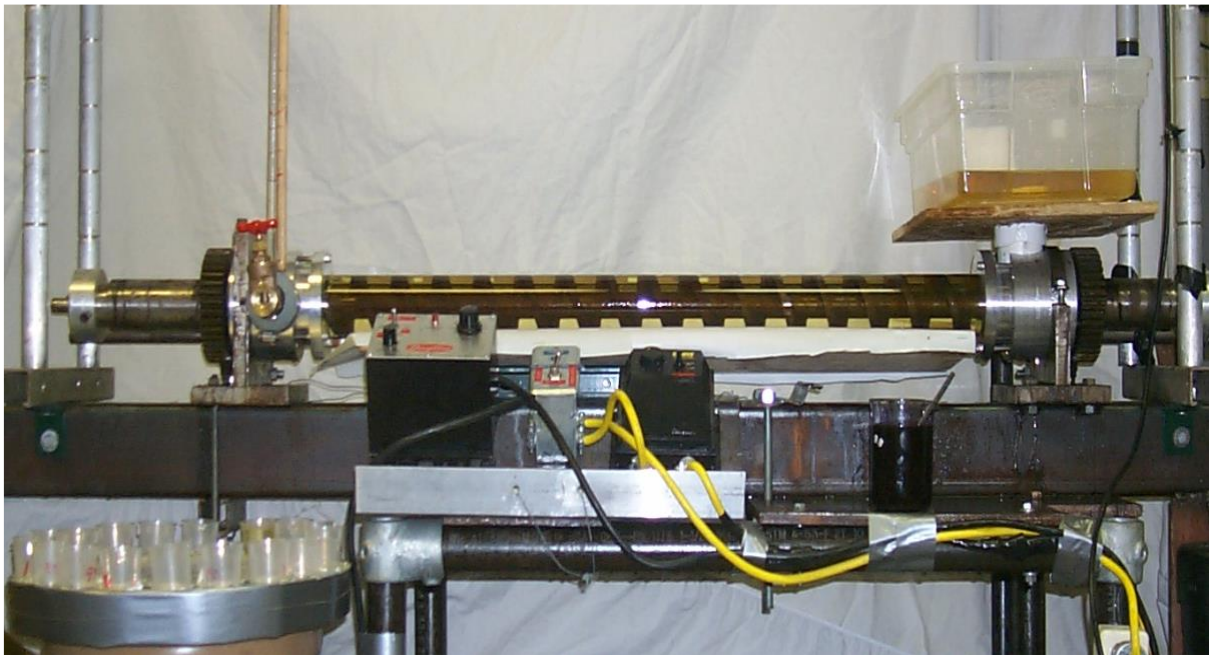

Figure 3. Clarkson Free Helix-Flight Extruder[15].

Figure 4 shows a schematic of this extruder and the unwound channel of the extruder with annotation letters that indicate how positions in the helical channel appear in the unwound channel. The barrel is stationary and appears to be moving to an observer located on a Cartesian coordinate system attached to the helix, as depicted in Figure 2. The observer, thus, appears to be stationary when either the flight-helix is rotated, or when the flight-helix and the core are rotated in the same direction at the same angular velocity, screw rotation. The motion of the screw pushes the fluid

up the channel in the Eulerian (laboratory) frame of reference. In the Lagrangian frame, the frame in which calculations are undertaken, it appears to the observer attached to the helix that the barrel is moving in the opposite direction, when the screw is rotated. For investigating chaotic mixing, utilizing this transformation from the Eulerian frame to the Lagrangian frame[17] would not result in a change in the physics or engineering fundamentals of the process, as discussed earlier. Our experimental device is not consistent with the shallow channel approximation, thus, the solution developed here is based on screw rotation physics discussed above instead of the historic barrel rotation analysis that is restricted to shallow channels.

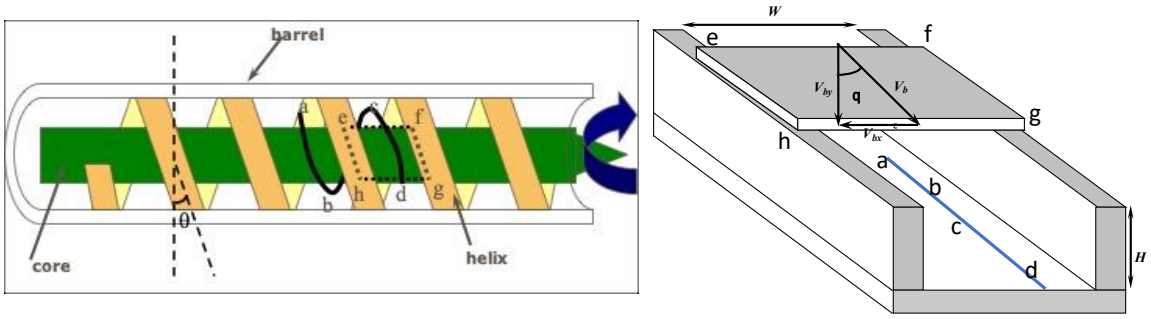

Figure 4. Diagram of the free helix extruder, fixed barrel, rotatable helix, flight and rotatable core, also referred as the screw root. Letters in left side image map to positions shown at right.

Many authors have investigated Stokes flow in a rectangular cavity induced by the motion of one of the walls. It has been shown that a biorthogonal series can be used to obtain an analytical solution for the biharmonic Stokes flow problem[18]. A similar analytical method was used to obtain the shape of corner eddies very accurately[19]. Also, a semi-analytical method was developed and used to obtain the streamlines for a deep channel as well as the streamlines in the multiple eddies that result[20]. Previously, an analytical solution involving two Fourier Series was used to obtain the flow field numerically and was used to compare data and calculations of the residence time of single screw extruders[21,22]. This method is computationally straightforward, gives accurate values of velocities, and accurately predicts the shape of corner eddies.

There has been some interest in the limitations of published simulations[23] and of mixing in cavities[24,25]. Some industrial practitioners have protected their intellectual property regarding chaotic mixing with a patent[26]. One of the earliest papers that focused on chaotic mixing was Aref's investigation of chaotic advection[27]. Chaotic mixing was also reported in rectangular cavity flows by the periodic motion of the top and bottom walls of the channel[28], in cylindrical cavity flows[15], by the periodic rotations of two co-rotating discs and in stirred tank reactors, and experimentally by changing the angle of the impeller with respect to the vertical[16,29]. Chaotic flows were studied computationally by dynamic flow perturbation using time dependent rotations per minute (RPM)[17]. In stirred tank reactors, the positions of the segregated regions were dependent on the impeller rotation rate where a fluctuation in the rotation rate led to widespread mixing. Thus, chaotic flow was generated when time-dependent RPMs were applied[30]. Mixing quantities for Stokes flow in a single screw extruder demonstrated that the growth of the interface between two substances are a linear function of time[22]. Deterministic chaos can be introduced into the extruder channel flow by making the flow field periodic. Mixing becomes an exponential function of time in the presence of this chaotic flow. Ottino et al. have shown that exponential mixing in two dimensions can be attained in a rectangular box, where both the top and bottom walls of the box move in a periodic fashion[23]. A reported numerical study of chaotic mixing in a rectangular cavity showed that there are mixing windows within the parameter space, where high quality mixing occurs[24]. There has been a renewed interest in the past few years in chaotic mixing with the single and multiple screw extruders[31,32,33,34,35,36].

With the increased degree of freedom in a free-helix extruder per Figure 3, it is possible to make the flow field chaotic by moving the core and helix in a periodic fashion. This is a different approach to that taken by Kim and Kwon[31,32], who showed that the three-dimensional channel

flows could be made chaotic by introducing spatially periodic barriers in the channel to break the cells. The screw that was used for this purpose was called "Chaos Screw". Instead of one elliptic point, an extruder with a barrier had two elliptic points and one hyperbolic point, a saddle point between the baffle and the top wall, in the cross-section of the extruder channel.

Experimental and numerical evidence for chaotic mixing in the free-helix extruder is presented here. The research presented here was undertaken in the Clarkson University Polymer Processing Laboratory using the free-helix extruder[37,38,39]. The flow field in the free-helix extruder was three-dimensional. Operating as a continuous process, the length of the screw limited the time available for mixing at any given flow rate. Conversely, a three-dimensional rectangular box and a batch stirred tank have no time constraints for mixing.

Simulating Chaotic Mixing in the Free-Helix Extruder

The free-helix extruder is a device in which we can obtain 3D chaotic mixing by making the top (barrel), and bottom (core) walls move alternately (as viewed from a frame of reference attached to the helix). Simulations of the flow in this device can be found from the method developed recently by Campbell et al[6]. The reader is referred to that paper for complete details of the calculation procedure. For discussion here, the equations labelled with ()* in the Model Development section are duplicates of those found the above reference and the numbers are maintained to aid the reader when utilizing to referenced paper.

MODEL DEVELOPMENT

The Stokes flow assumption used in this analysis is appropriate because of the high viscosity of molten polymers which generally leads to a Reynolds Number less than 1.0. The

equation for the Stokes flow of a Newtonian fluid in the rectangular cavity in the *transformed (moving) reference frame* shown in Figure 2 is given by:

$$\frac{\partial P}{\partial x} = m\left[\frac{\partial^2 V_x}{\partial x^2} + \frac{\partial^2 V_x}{\partial y^2}\right] \qquad (1)^*$$

$$\frac{\partial P}{\partial y} = m\left[\frac{\partial^2 V_y}{\partial x^2} + \frac{\partial^2 V_y}{\partial y^2}\right] \qquad (2)^*$$

$$\frac{\partial P}{\partial z} = m\left[\frac{\partial^2 V_z}{\partial x^2} + \frac{\partial^2 V_z}{\partial y^2}\right] \qquad (3)^*$$

Eq. (3)* describes the down-channel flow. Eqs. (1)* and (2)* can be combined and solved as a two-dimensional, cross-channel flow field. To solve the equations, a stream function, ψ is introduced. The boundary conditions for solving Eqs. (1)* and (2)* in terms of ψ are given by

$$\frac{\partial \psi}{\partial x} = 0 \ , \ \psi = 0 \quad \text{at } x = 1 \qquad (5a \text{ and } 5b)^*$$

$$\frac{\partial \psi}{\partial x} = 0 \ , \ \psi = 0 \quad \text{at } x = -1 \qquad (5c \text{ and } 5d)^*$$

$$\frac{\partial \psi}{\partial y} = 0 \ , \ \psi = 0 \quad \text{at } y = 0 \qquad (5e \text{ and } 5f)^*$$

$$\frac{\partial \psi}{\partial y} = -1, \ \psi = 0 \quad \text{at } y = b \qquad (5g \text{ and } 5h)^*$$

A stream function equation can then developed and is written as

$$\frac{\partial^4 y}{\partial x^4} + \frac{\partial^4 y}{\partial y^4} + 2\frac{\partial^4 y}{\partial x^2 \partial y^2} = \nabla^4 y = 0 \qquad (6)^*$$

where the operator ∇^4 is called the *biharmonic operator*. All lengths are non-dimensionalized by dividing by the half channel width (in this case that is set to 2) as shown in Figure 5.

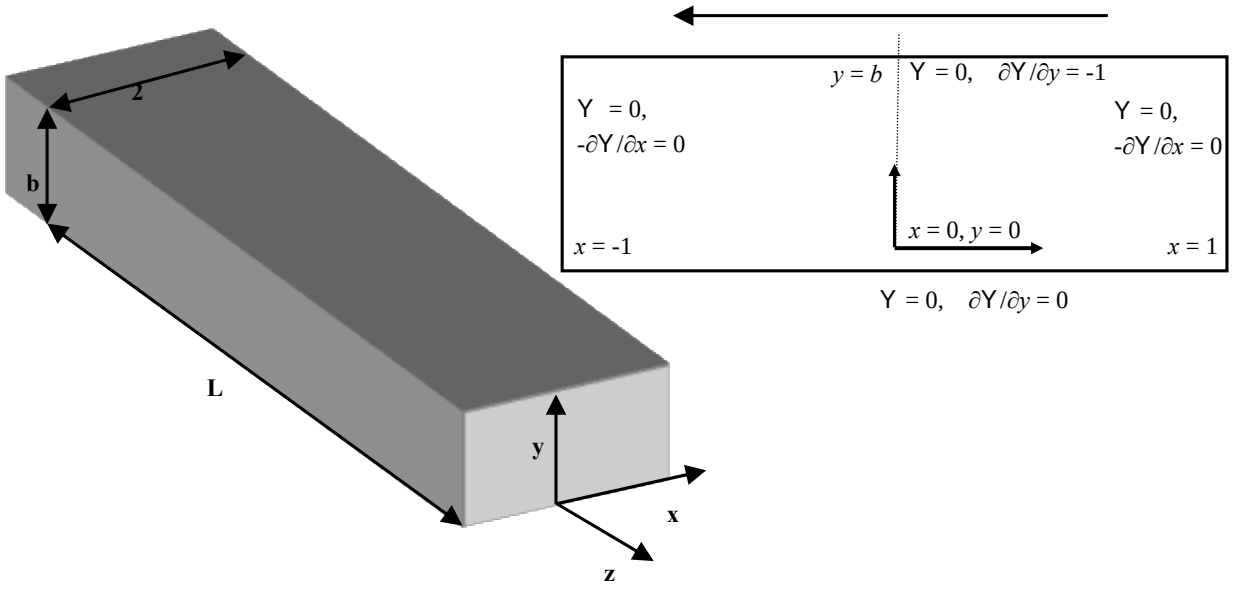

Figure 5. Non-dimensionalized rectangular channel, $b = H/W$ is the aspect ratio of the channel. The top wall is moving with velocity of -1. The image upper right shows the stream function boundary conditions at the cavity walls.

This produces the following three sets of equations[Error! Bookmark not defined.] :

$$\left[a_m Y_m'(b) + \sum_{n=1}^{\infty} (-1)^n a_{m,n} \times \left(\frac{n\pi}{b} \right) \times b_n \right] = 0 \qquad (16a)^*$$

$$\left[-c_m Y_m'(b) + \sum_{n=1}^{\infty} a_{m,n} \times \left(\frac{n\pi}{b} \right) \times b_n \right] = 0 \qquad (16b)^*$$

$$\left[b_n X_n(1) + \sum_{m=0}^{\infty} b_{n,m} \left(a_m + c_m (-1)^{n-1} \right) (-1)^m \right] = d_n \qquad (16c)^*$$

The above set of equations is not finite. Both the subscripts m and n go to infinity. Eqns. (16a)* to (16c)* are truncated at $n = N$ and $m = M$ to obtain a finite set of $2(M+1)+N$ equations in as many unknowns. These finite set of linear equations are solved by the LU-Decomposition method.

Returning to the derivation in the present work, the particles in the flow field can be tracked by:

$$x(t+\Delta t) = x(t) + V_x \times \Delta t + \frac{1}{2} \times a_x \times \Delta t^2 \qquad (3.a)$$

$$y(t+\Delta t) = y(t) + V_y \times \Delta t + \frac{1}{2} \times a_y \times \Delta t^2 \qquad (3.b)$$

$$z(t+\Delta t) = z(t) + V_z \times \Delta t + \frac{1}{2} \times a_z \times \Delta t^2 \qquad (3.c)$$

where,

$$a_x = V_x \frac{\partial V_x}{\partial x} + V_y \frac{\partial V_x}{\partial y}$$

$$a_y = V_x \frac{\partial V_y}{\partial x} + V_y \frac{\partial V_y}{\partial y}$$

$$a_z = V_x \frac{\partial V_z}{\partial x} + V_y \frac{\partial V_z}{\partial y}$$

Testing the Model

Mixing characteristics, residence time distribution and particle trajectories can be obtained by tracking particles in the flow field. For these simulations the free helix extruder was modeled in three modes: screw rotation, helix rotation, and chaotic rotation. Results for these calculations are shown in Figure 6. The screw rotation and the helix rotation need about the same length of time to reach the maximum exit concentration, this is consistent with the discussion above relative to equation 2. The screw rotation has the traditional long tail while the flight-helix rotation has essentially no tail. This is because there are no stable Moffat eddies due to there being no "dead" corners when the flight-helix is rotated. The results of the simulation of chaotic boundary conditions have a longer mean residence time and a broader time dependent distribution, indicating better mixing.

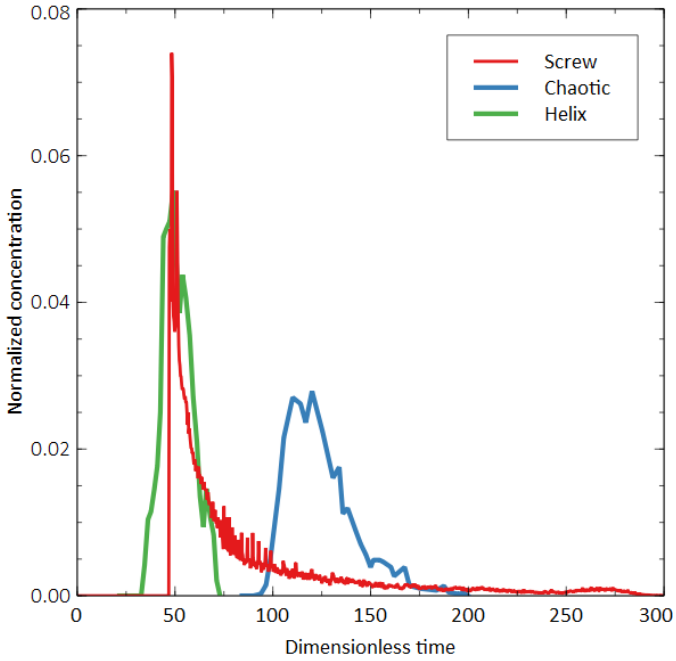

Figure 6. Predicted Residence Time Distribution for three screw rotation modes[37,38,39].

It is also possible to pump fluid simply by rotation of the core. However, this produces a small output, m^3 per revolution, and was not done as part of this investigation. Model streamlines for two modes of operation are shown in Figure 7. When only one wall is moved, a single fluid rotation cell is developed as shown in the right plot in Figure 7. More detail including the Moffat eddy from using the model in this mode can be seen in Figure 1. In this case, details of the flow in one of the corners shows the existence of a Moffat eddy as shown in Figure 1 but not in Figure 7. When both the top and bottom walls are moved, representing the flight-helix rotation, there are two fluid rotation cells of streamlines as seen in the left plot in Figure 7.

To further evaluate the model characters, three different flow patterns are analyzed: one for a traditional laminar flow and two for chaotic flows:

1. Normal laminar flow pattern in a single-screw extruder in which only the top wall is moving.

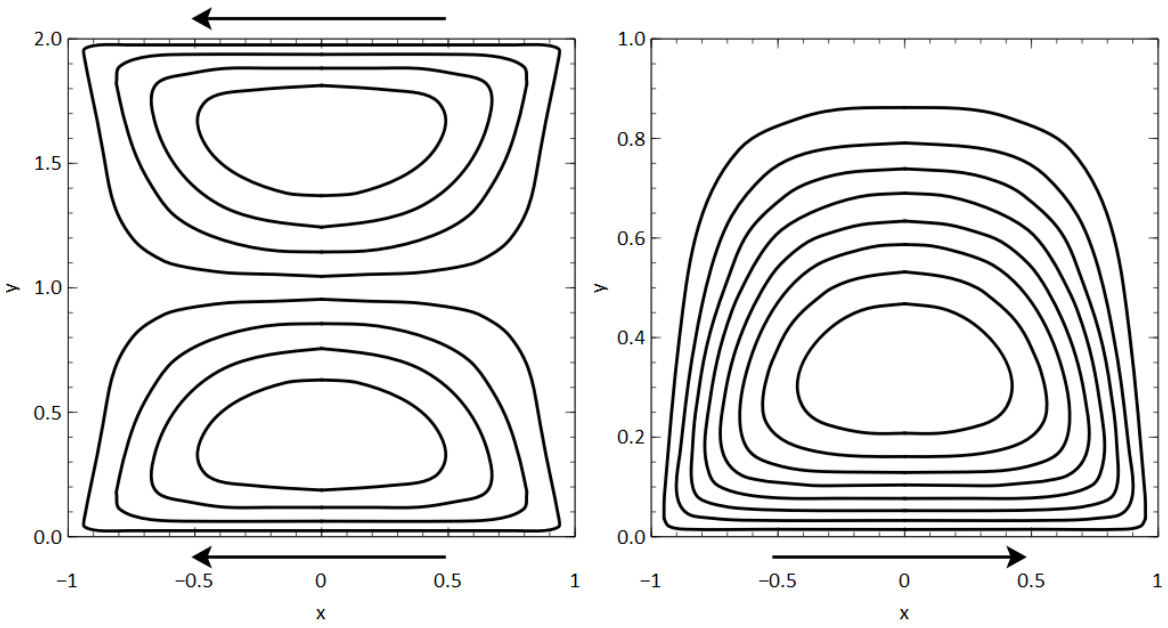

Figure 7. Streamlines obtained using this analysis. The left plot has both top and bottom walls in motion with height to width ratio of 2; the right has only the bottom wall moving with height to width ratio of 1. Arrows show direction of motion of the walls.

2. Chaotic Pattern-1 in which the top and bottom walls of the rectangular channel alternately move in the same direction for some time. To obtain this pattern the helix and core are rotated together as a single screw for a period of T seconds. Then the core rotates in the opposite direction while the helix rests for another T seconds. From a frame of reference attached to the helix, it will appear as though top (barrel) and bottom (core) walls are moving alternately in the same direction.
3. In what we call Chaotic Pattern-2, the flow pattern of Chaotic Pattern-1 is disturbed at regular intervals; every $2nT$ seconds only the helix turns in the forward direction for one period ($n = 2$ is used in all simulations discussed herein).

The simulations shown in Figure 8 are cross-sectional views of the three modes described above with $T = 4$ used in all simulations. Figure 8 shows the two-dimensional projection obtained

while looking along the z-direction of the channel. The two modes of chaotic deformation produce better mixing of the drop than the laminar deformation. Chaotic Pattern 2 distributes the drop's particles more homogeneously because the stream function produced by the motion of the helix involves two complementary circulation patterns.

The next test involves simulating the flow in the single screw extruder when four differently colored particles are conveyed from the melting zone into the pumping zone. A typical result with conventional laminar mixing is shown in Figure 9. It shows how four drops deform as they are displaced from their original locations. The four drops were initially placed as shown in the upper left rectangle in Figure 9. Looking down the channel, the deformed drops appear as shown in the lower left rectangle in Figure 9. The three-dimensional figure to the right shows how the drops have stretched and moved down the channel. With this conventional laminar stretching of the fluid particles there is almost no effective mixing of the four drops; they remain isolated.

Figure 9 showed the mixing of four drops when the top and bottom surfaces moved as required by conventional screw rotation. The very small displacement of the red drop suggests that it very quickly approached the wall and saw only very small velocities. The drops in Figure 10 had the same initial placement as did those in Figure 9. Again, the lower left-hand element in the figure is what would be observed when looking down the channel after the mixing motion had ceased. The particle blobs are now well distributed over the entire cross-sectional area of the channel. The right-hand plot of Figure 10 demonstrates that the blobs have not only been well distributed across the area of the channel, but these blobs have also dispersed in an essentially random manner to fill the length of the channel. Qualitatively, this is much better mixing than that shown in Figure 9

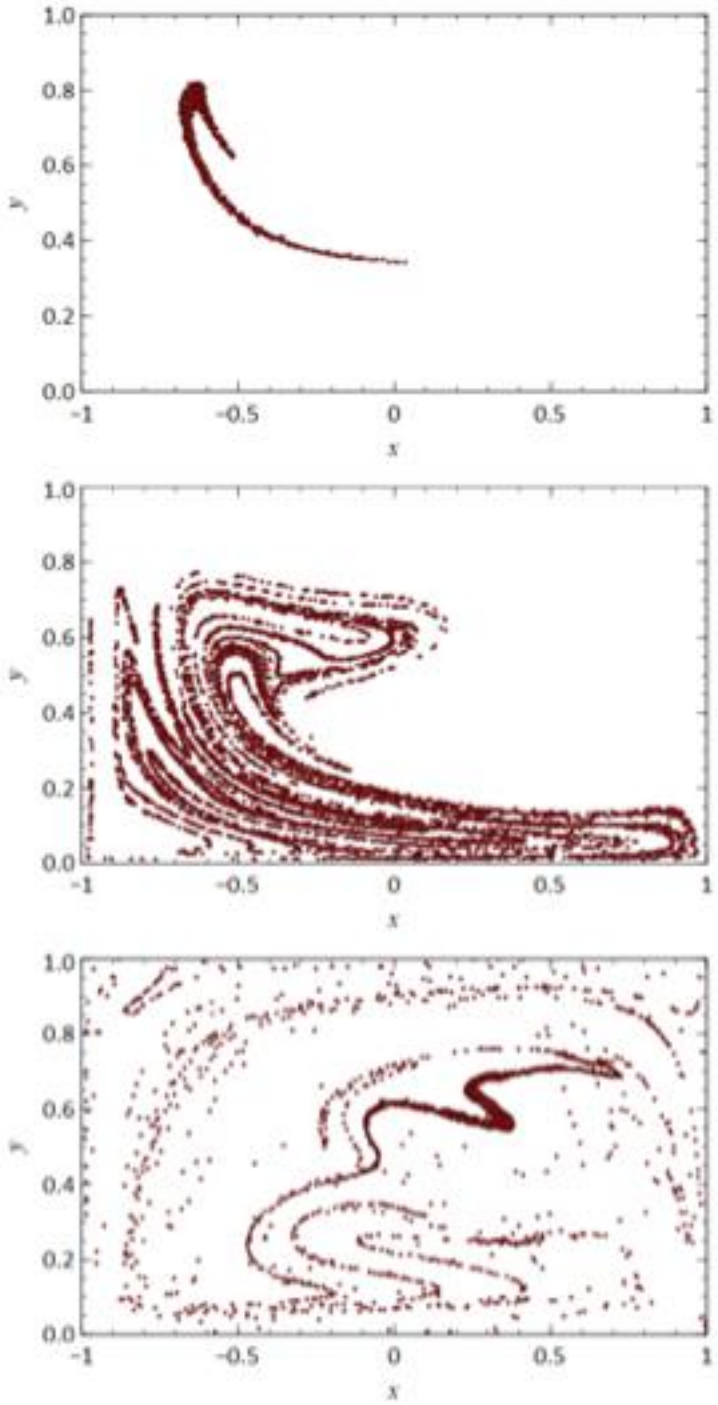

Figure 8 Simulations of drop deformed by three different mechanisms: Top shows laminar displacement, center shows chaotic pattern 1, bottom shows chaotic pattern 2 (see text for explanation)[39].

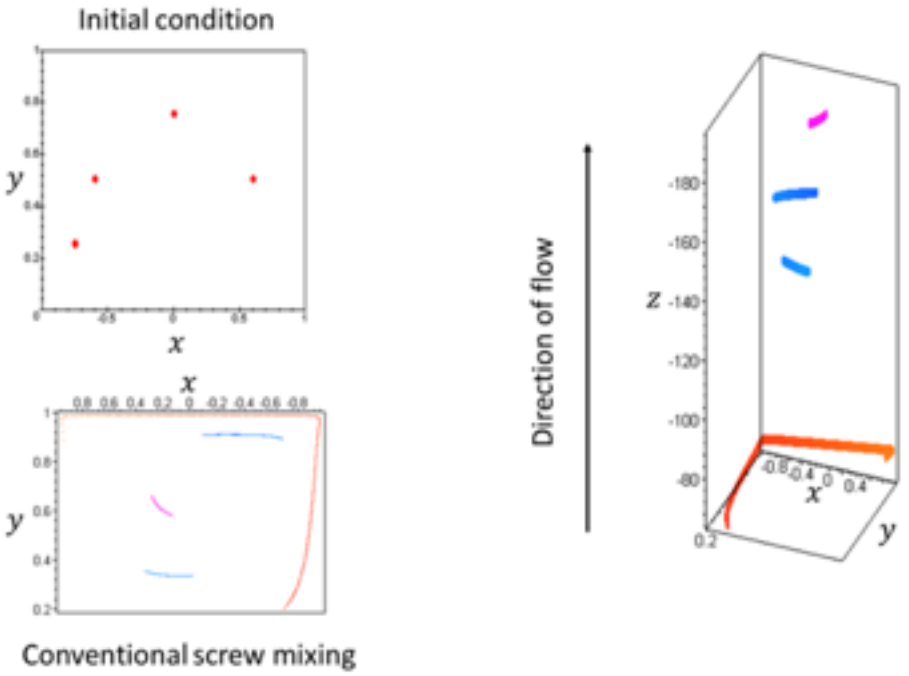

Figure 9 Mixing of color blobs with laminar flow in a screw channel assuming conventional screw mixing. The top left shows the initial position of the colored blobs. The top wall of the extruder is in motion for this simulation[39].

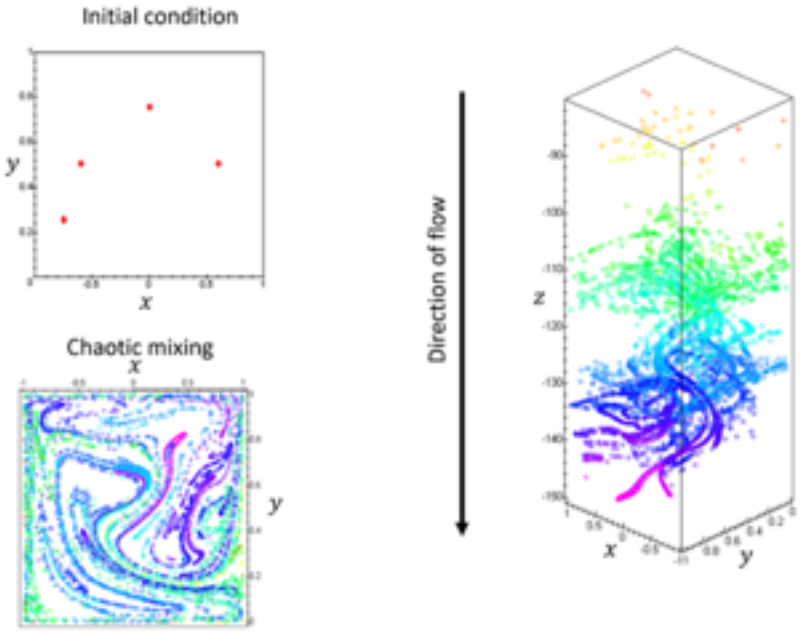

Figure 10 Mixing of four drops in a screw channel driven by chaotic deformation. The arrow indicates direction of flow. The number of particles is 1600 of each of four colors. The duration of simulation is 100 seconds, VB = 1 M, Period = 4 s [39] .

EXPERIMENTAL SECTION

A schematic diagram of the extruder and data collection system is provided in Figure 11. A photograph of the extruder and dye analysis set up was shown in Figure 3.

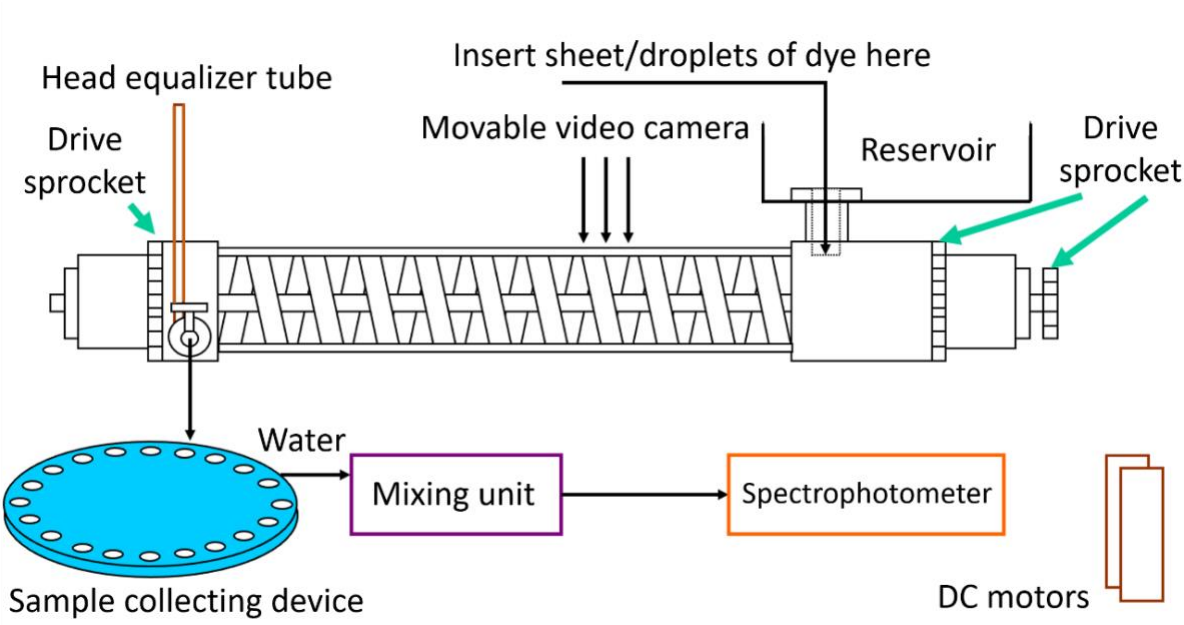

Figure 11. Schematic of the data collection system.

As pointed out earlier, to get the degrees freedom required to produce chaotic mixing, the extruder screw was designed such that the screw flight-helix was a separate and independent of the screw core. The barrel of the extruder was made of extruded glass polished to a 0.059 m inside diameter. Inside the glass barrel, the helix was constructed of steel which was detached from the core. The fit of the helix had minimum clearance to both the barrel and the screw core. This minimized leakage as did keeping the pressure drop as close to zero as possible during the runs. Unlike most screws that become narrower as the flight goes from the barrel to the screw root, the free helix was machined so that the walls were vertical. Thus, the channel width was taken as $2W$

to be consistent with the boundary conditions per Figure 5, which was effectively constant from the top to the bottom of the flight. The helix was driven from both ends by sprockets with the larger sprockets in Figure 11 attached by a chain to a sprocket on a gearbox which was attached to a 5 W DC motor drive. The helix was driven at both ends to prevent a spring-like longitudinal contraction and radial expansion near the midsection. With the required tight tolerances, this deformation would cause the helix to bind or cause it to rupture the glass barrel. The core was a steel shaft that was driven at one end by another sprocket attached to a separate 5 W DC motor drive. Both the helix and the core could be turned independently clockwise or counterclockwise with the reversible drives. Sealed bearings at the ends allowed the core to rotate within the mounts of the helix with no fluid leakage. If these two screw elements were rotated in the same direction at the same angular velocity, the device functioned as a conventional single screw. The elements were operated independently to induce chaotic flow in the channel. The extruder, working fluid, and process functions are detailed in Table I and Table II.

Table I Specifications of the extruder

Extruder Parameter	**Value**
Length of the barrel:	105 cm
Outer diameter of the barrel:	6.8 cm
Helix diameter:	5.92cm
Core diameter:	2.34 cm
Flight height, H:	1.79 cm
Distance between two flights:	5.5 cm
Flight thickness (at Barrel):	1.1 cm
Channel thickness (Parallel to core at barrel):	4.4 cm
Helix angle:	16.5 degrees
Width of the channel 90^{o} to Flights; 2W=:	4.29 cm
Average radius of the channel:	4.13 cm
Length of the channel per turn (using average radii):	14.06 cm

The working fluid was a The Dow Chemical polypropylene oxide Polyol, a secondary hydroxyl high viscosity Newtonian polymeric liquid.

Table II Processing - Material Specifications

Parameters	**Value**
Polyol Viscosity (μ)	65.96 poise
Polyol Density (ρ)	1.015 kg/m^3
Screw Velocity (V) at Barrel Interface	1.75 cm/sec
Characteristic length (D_e)	8.26 cm
Reynolds number ($N_{Re} = D_e V\rho/\mu$)	0.2224

The process Reynolds number was less than 1 consistent with the model assumptions. The feed inlet was situated over the top of the barrel about 2 turns of the helix ahead of the helix mounting point. The feed orifice was slightly smaller in diameter than the inside diameter of the barrel. It was equal in width to the lead of the helix. A fluid reservoir with a large cross-sectional area was mounted above the inlet and was designed to minimize the inlet pressure change by spreading the fluid out over a large surface. This served to minimize the pressure head change during the run by decreasing the height change of the reservoir. The outlet design was the same as the inlet but was attached to the side of the barrel. A conical restriction was designed for the outlet to accelerate the streamlines evenly and to minimize the amount of mixing as the fluid exited the extruder channel. The fluid passed through a gate valve used to regulate flow at the outlet. A "capillary" fixed to the end of the extruder was filled with the working fluid above the extruder and acted as a pressure gauge at the outlet immediately preceding the gate valve. This arrangement allowed the operator to regulate the pressure head at the outlet of the extruder by adjusting the gate valve while collecting the extruded fluid samples. For this investigation, it was desirable to keep the capillary height at the same level as the fluid in the reservoir, thus having no pressure gradient across the working length of the extruder.

General Procedure

The general experimental procedure will now be described. The only difference between runs was a change in the mixing pattern between modes of operation. For the first set of experiments, a concentrated solution of crystal-violet dye was mixed with some Polyol and injected at the entrance of the extruder with a syringe and a transfer needle. At the time of injection, the colored blob was about 2mm in diameter. The extruder channel had an aspect ratio of about 0.85 and was 2.5 cm deep. Typically, any screw with an aspect ratio of about 0.1 is considered a deep channel screw.

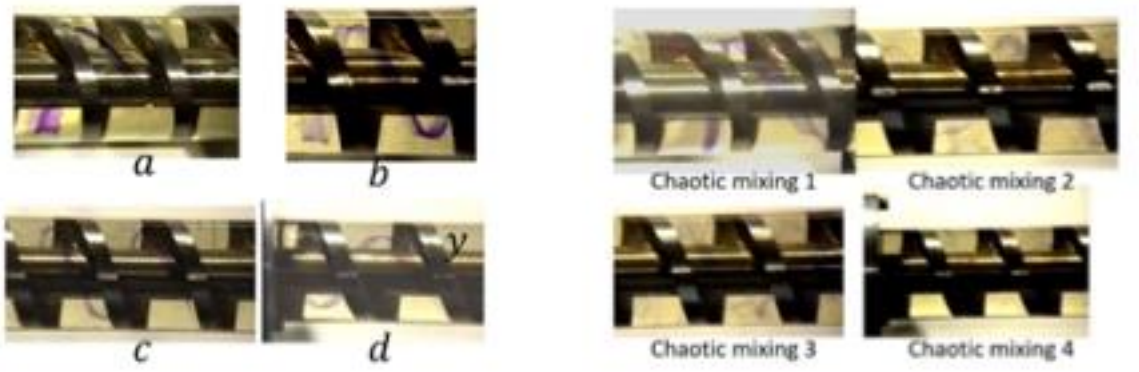

Figure 12. Comparison of dye blob deformation for both screw and chaotic velocity fields. Conventional screw rotation is shown in the four left-side images. Chaotic mixing screw rotation is shown in the four right-side images.

Figure 12 shows the deformation of a blob for both the conventional screw rotation mode and a chaotic mode in the glass-walled extruder. The blob was introduced under the square reservoir shown in Figure 3 and Figure 11. The four sequenced photos for the screw and chaotic rotation modes were taken as close as possible to the same position on the extruder during the tests. By the time it becomes visible in Figure 12 (a) and Chaotic mixing 1, it has been stretched to a certain degree.

In Figure 12 (b) the blob has been stretched and flattened into a tape like structure. As the blob proceeds down the extruder channel, Figure 12 (c), it continues to stretch.

In Figure 12 (d) the dye has moved into a part of the channel where the previous tape like stretching has essential reversed, and the dye exits the extruder as an almost intact helical string like structure.

This screw mixing dynamic is now compared by using the free helix extruder as a chaotic mixer. To induce chaos into the flow field, the rotation of core and helix was made periodic. The core and helix were rotated in the forward direction for 10 seconds, and then only the core was rotated in the opposite direction with same surface velocity as produced at the barrel screw barrel interface for next 10 seconds (this is Chaotic Pattern-1). This gave rise to a periodic and essentially constant average flow rate towards the outlet of the extruder. The rotational flow within the extruder channel alternating directions produces what is referred to as deterministic chaotic mixing that is responsible for the blob breaking into smaller pieces, each becoming stretched into minute strands. Clearly the chaotic pattern sequence on the right side of Figure 12 shows much better mixing than the normal laminar screw mixing pattern on the left side of Figure 12.

The dynamics of the changes in the dye blob for the chaotic case show that with chaotic mixing the blob appears to be broken up.

Figure 12 (Chaotic mixing 3) shows what appears to be the Baker's Fold of the dye.

This is one of the classic techniques used for producing chaotic mixing. In the Figure 12 (Chaotic mixing 4), the dye has become so well dispersed and is so faint that it is hard to determine where it begins and where it ends: this is the same physical position as d for the screw sequence on the left side of Figure 12.

It was determined that syringe injection of the dye did not provide quantitative data for comparison with the computational results, so a different dye insertion technique was developed. Frozen tracer dye was positioned at the entrance to the extruder (additional detail is provided below). This technique provided accurate dye placement, so the experimental and computational results could be compared. Once the tracer dye thawed, the extruder was operated using the residence time mode of operation. It was not necessary to collect samples until the dye was near the outlet which was easily determined from visual inspection through the glass barrel. However, it was important to be sure that at least two samples were collected with no dye visible immediately before the dye began to come out. These samples were used as blanks during analysis for the calibration of the spectrophotometer. Calibration curves had been prepared using a spectrophotometer by collecting the UV-Vis absorbance readings for known concentrations of crystal violet dye in polyol. The UV-Vis absorbance readings were then recorded for all the samples and compared to concentration calibration curves to determine the total amount of dye so that the RTD can be calculated.

Another issue to be considered when trying to quantify the difference in the two mixing regimes, was the reproducibility of placement of the blob of dye, in the rectangular channel. If the blob was placed in a low mixing region, the mixing obtained by Chaotic Mixing Pattern-1 would not be as effective as that seen in Figure 12.

When the extruder was operated as a normal single-screw extruder, the blob was stretched into a long streak with minimal mixing in the carrier fluid. In the chaotic flow field, the blob was split into minute strands becoming nearly invisible at the outlet of the extruder. It was also a challenge to place the digital particles correctly in the simulations for comparison with the

experiments using the traditional down-channel fluid mechanics model combined with the new solution of the biharmonic equation.

A technique to reproducibly place the dye in the extruder was developed to address these issues[38]. For the experiments to be effectively compared to and test the simulations, it was considered desirable to have two dye structures that could be reproducibly simulated with digital particles. A thin sheet of dye that spanned the screw channel normal to the flight-helix, a close approximation of a Dirac function, and a set of droplets/discs were used. The reproducibility of placement of tracer dye droplets/discs was a vital part of the experiment and allowed effective simulation comparison with the conventional and chaotic mixing using Residence Time Distribution (RTD) simulations.

There have been many different techniques used for determining the exit concentrations of a tracer in order to calculate the RTD in extruders. Another robust technique when extruding polymers is to use TiO_2 nanoparticles as the tracer because they are detectable at very low concentrations using infrared analytical techniques[40]. Bur[41] used a florescent dye and a continuous monitoring probe to measure RTD in a twin-screw extruder. Since the twin screw extruder has mixing elements and the channel sides are essentially parabolic, the assumption that the probe is measuring the average dye concentration was considered to be sufficient. This is not the case in the single screw extruder as seen in Figure 12.

Because of the segregation of the dye in the experiments, it was necessary to mix the samples after they were collected at the extruder exit.

Using a syringe, either a sheet or drops of crystal violet dye mixed in Polyol were placed where desired on the frozen sheet of Polyol already in the box as illustrated in Figure 13. Schematic showing the aluminum foil mold used to make the dye sheet and droplet

"sandwich"[38]. The drops spread into thin discs that more closely resemble the placement of the digital particles at $z = 0$ during the simulations. The two structures sat momentarily so that they would bond slightly. The sandwich was frozen for a final time and placed into the extruder screw channel with tongs so that the crystal violet sandwich was perpendicular to the screw flights. The details of this procedure may be found in Campbell et al[6].

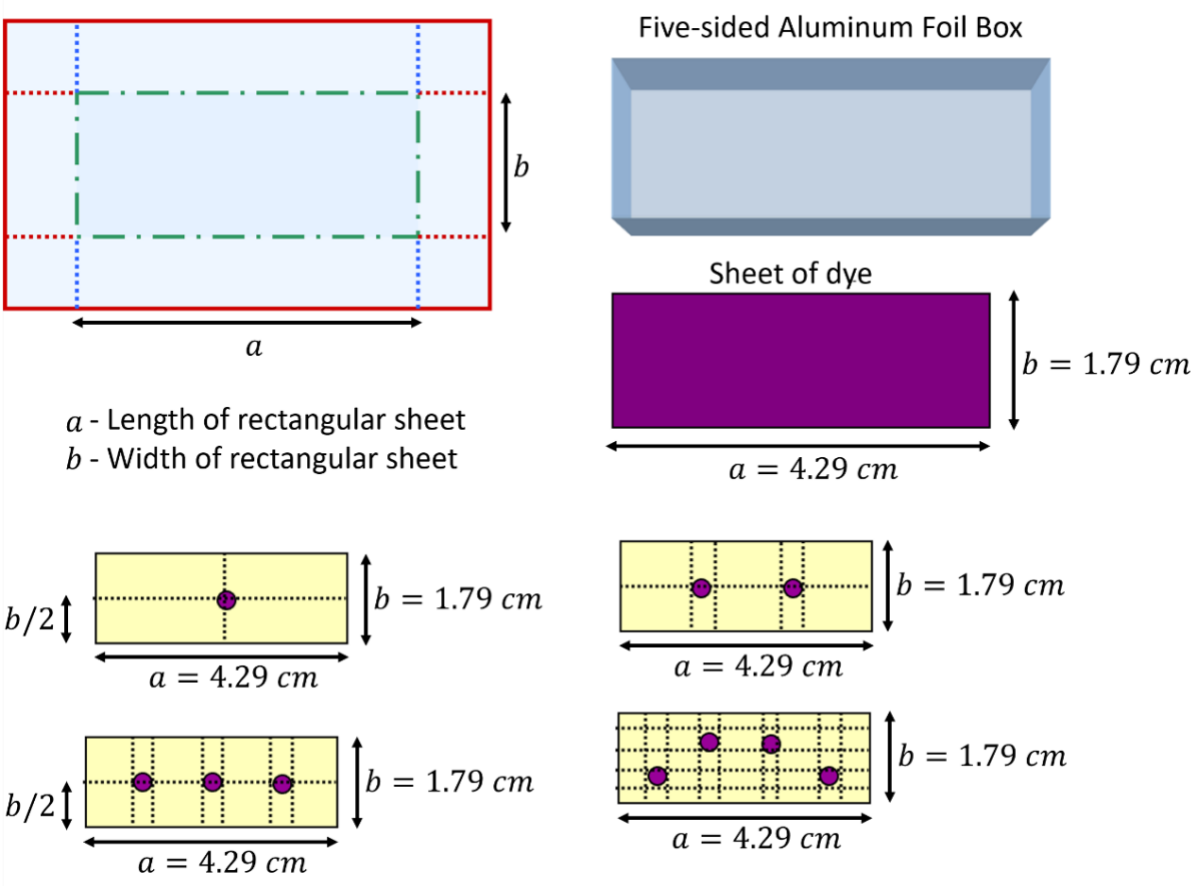

Figure 13. Schematic showing the aluminum foil mold used to make the dye sheet and droplet "sandwich"[38].

In order to compare the experimental and computational results, the dye had to be placed at the entrance of channel consistent with the initial boundary condition of the simulation shown in Figure 14. Quantitative comparisons for experiments and simulations of screw rotation and

chaotic mixing in the free-helix extruder were now possible. Figure 15 shows a comparison of the experimentally determined and simulated RTD for a conventional screw rotation. The RTD was determined experimentally using a dye sheet input and measurement of the concentration of the crystal violet with a UV/visible spectrometer.

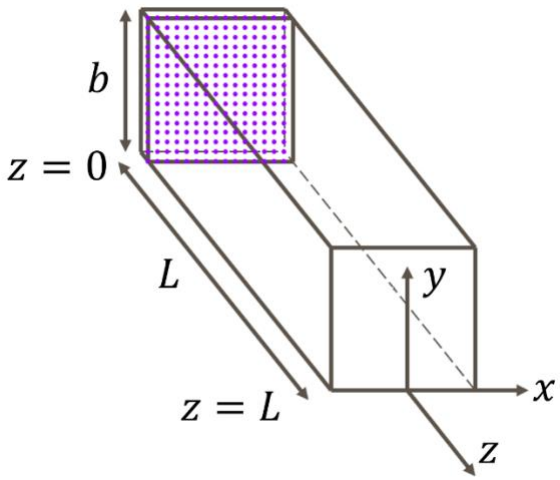

Figure 14. Representation of particle placement for simulation of sheets, each sheet had 400 × 400 particles.

The simulation started with 16,000 digital dots homogenously distributed at the beginning of the rectangular screw channel, $z = 0$. The drops/discs were nominally 0.45 cm in diameter. The digital dots were allotted to the drops/discs or the background when the drops/discs were being simulated.

Quantifying Residence Time Distribution

Flux of particles entering at point (x, y) in the cross section is proportional to the velocity at that point. The mean residence time calculated from the exit age distribution is equal to the space-time. The equation that defines the concentration distribution function is:

$$f(t) = \frac{N(t, t+\Delta t)}{N_0} \tag{3}$$

f(t) is the normalized concentration. It is the fraction of particles or dye exiting the channel with a residence time between *t* and *t*+Δ*t*. *N*(*t*, *t*+Δ*t*) is the number of particles with residence time *t* and *t*+Δ*t*. N_0 is the total number of particles or dye recovered at the end of the channel; it represents the integrated sum of all the dye or the particles that make it to the end of the channel, there is often a digital loss of a few particles through the boundary.

The other function required is the non-dimensional time that relates the experimental particle space time to the simulation space time with *R* = 2.065 cm and *W* = 2.11, the half width of the channel consistent with the boundary conditions in Figure 5. "*T"* is the process sample time. The screw rotation rate at the barrel boundary is calculated from

$$v = \frac{2\pi(2.065\text{cm} \times 8.1\text{RPM})}{2.11\text{cm} \times 60\text{sec/min}} = 0.829719\frac{1}{\text{sec}} \tag{4}$$

The rotation rate using the flight-helix angle is

$$v_z = v\sin(0.28767\text{rad}) \tag{5}$$

The non-dimensional time is then calculated for each digital or experimental sample by

$$t = v_z T \tag{6}$$

The comparison of simulation and experimental results presented in Figure 15 (left) shows that both possess two major peaks early as the dye exited the extruder and a long tail that is characteristic of single screw dynamics due to the existence and domination of the Moffatt eddies shown earlier in Figure 1. The experiment involves a transient start whereas the model assumes steady state. This transient startup appears not have substantially affected the results because the

experimentally observed and computed distributions match the timing of the multiple maxima in the RTD function. The minimization of any transient startup effect is probably due to the high viscosity of the fluid and the almost instantaneous rotation rate due to the drive system.

Simulation and experimental results were also compared for Chaotic Pattern-1 in Figure 15 (right). In the numerical simulations, the top wall and the bottom wall of the rectangular channel were moved alternately in a direction opposite to that of the flow in the channel. There is substantially less of a tail in either the simulated or the experimental distributions for this type of motion. This is because the plane of motion was changed periodically (alternate direction of motion of the top and bottom walls), thereby periodically destroying the corner (Moffatt) eddies that cause the long tail in the screw motion. During the screw motion part of the cycle, the Moffat eddies would be expected to again form. Corner eddies were formed in the bottom of the channel in the screw motion and in the top of the channel in the core motion. Periodically alternating the direction of motion destroys the corner eddies during that part of the cycle. This leads to the material in the corners encountering other parts of the channel and, hence, gives rise to more mixing because the material in the essentially static zones that cause the Moffatt eddies has been distributed throughout the fluid in the channel.

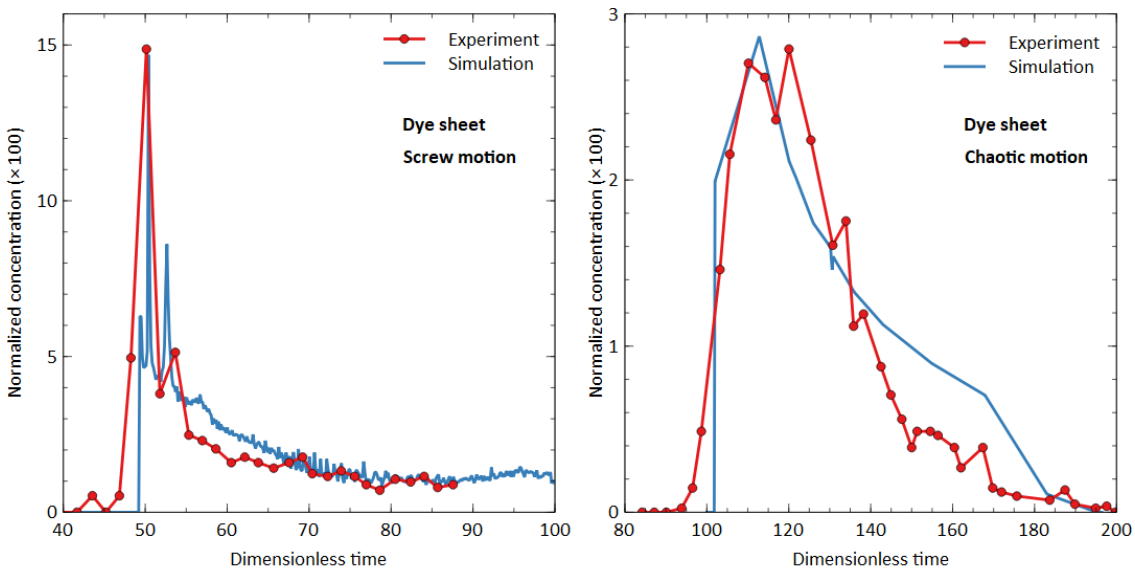

Figure 15. Residence time distribution for the dye sheet: Left is the conventional screw rotation mode[39]. Right is chaotic motion in the free helix extruder[37,38].

By comparing the results for the RTD of a sheet using conventional screw and chaotic motions seen on both sides of Figure 15, it can be seen that the dye begins to exit the extruder sooner when in screw motion. This is due to the backward movement of the core alone in the chaotic motion, which gives very little output (the flow rate was decreased to maintain a near-zero pressure gradient). Thus, it takes longer for the dye to reach the exit of the extruder when in chaotic motion. For the maximum in the *f(t)* concentration as a function of time, the *y* coordinate function decreases for the chaotic mixing which corresponds to the increasing mixing efficiency, leading to a broader RTD function as compared with the screw motion. The half width of the major peaks during screw mixing was about 10*t* compared to about 30*t* for the chaotic mixing. The minimization of the tail that is present during chaotic motion would make color or grade changes in the extruder easier to accomplish.

In the polymer industry, the typical concentration of color concentrate added is less than 5% of the resin introduced into the extruder[4]. In order to evaluate this diluted mixing in the free-

helix, drops were evaluated relative to mixing mechanism. The screw RTD and the chaotic RTD were then compared for 1, 2, 3 and 4 flattened drops, refer to Figure 13, regarding the shape of the inputs for both the experiments and the simulations. The input for the drops was constructed and inserted into the extruder in the manner discussed above for the sheet of dye input. Typical results for these experiments and simulations are shown in Figure 16 and Figure 17. No long tail is visible in any of these RTDs because none of the drop(s)-disc(s), were in the area where the Moffatt eddies form. There were, in general, the same number of major peaks in the RTD as the drops-discs that were introduced. For 2 and 3 drops, there was a very short tail, but not as pronounced as one would expect from a response dominated by Moffatt eddies. The shift in mean exit time reflects the average down channel velocity encountered as the drops/disks traversed the channel, a function of their initial placement in the channel. The longer time from start to end of the 4 drop RTD suggests that this might be the minimum color concentrate concentration that should be utilized in commercial extrusion.

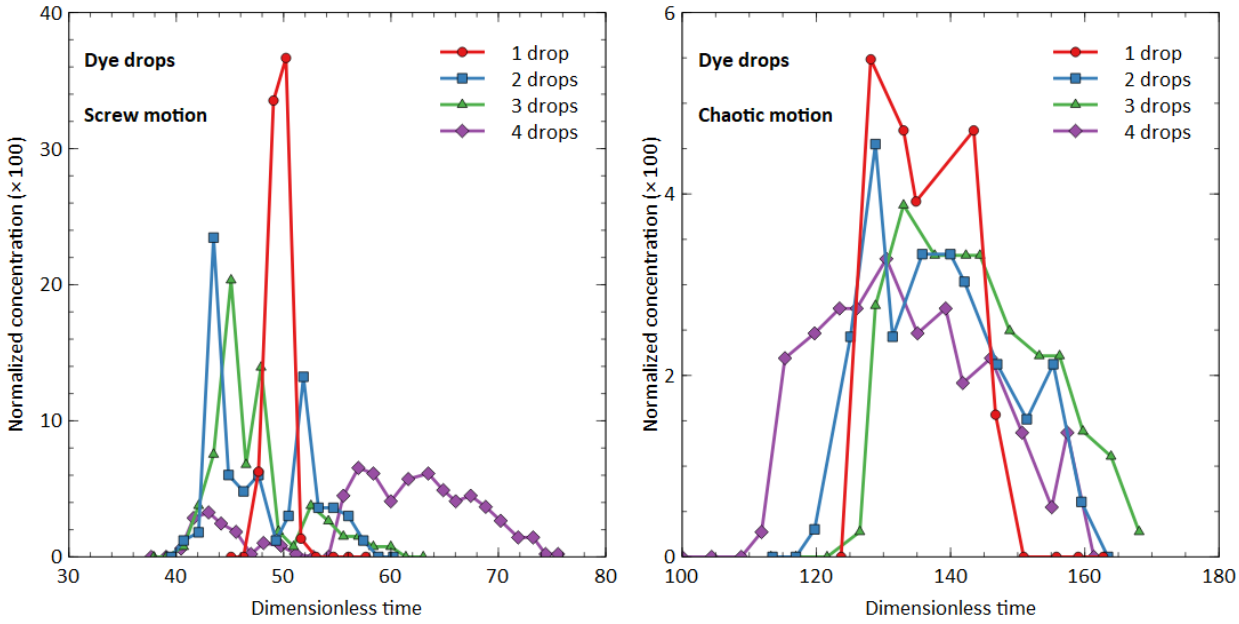

Figure 16. Experimental drop RTD for screw rotation (left) and for chaotic rotation (right).

For the equivalent chaotic mixing results for 1, 2, 3 and 4 drops, the *f(t)* function has a much lower maximum concentration, a longer residence time, and no long-term tail. There is no tail with four drops and the strong bimodality has vanished. Mean RTD exit time for the chaotic mixing was always longer than for the screw rotation.

For 1 drop screw rotation, both the experiments and the simulations produced similar RTD function width and exit time related to extruder exit time, 7 (top left). The screw rotation comparison has a small secondary peak for the simulation but no long tail. For chaotic mixing, the simulations provide a functional shape that is somewhat different when comparing simulation with the experimental data. The peaks are centered at the same exit time and have essentially the same half width for the distribution. However, the simulation does not have the strong second peak that is apparent in the experimental results. After the RTD midpoint, there are inflections in the computed results. These are not representative of the strong second peak from the experiment.

Even for the four-drop screw rotation RTD, both the experiment and simulation produce the bi-modal RTD function for screw rotation. In general, the multiple peaks from the experiments can also be found in the simulation results for screw rotation. This suggests that the analytical solution using the bi-harmonic equation developed by Campbell et al. quite accurately represents the flow in the rectangular channel[6]. For the 4 drops-discs, the chaotic simulation was semi-quantitatively representative of the experimental data. However, the simulation did not produce the peak detail associated with the last half of the experimental distribution function.

The comparison of the results suggests that the dynamic simulation captures the overall dynamics of the experimental results. However, some of the experimental details of the drop experiments are a semi-quantitative representation of the chaotic fluid mechanics of the screw

channel, Figure 17. The simulation grid was calibrated using screw rotation RTD. The apparent loss of detail in the last half of the chaotic RTD simulations may be due to our decision to keep the simulation grid constant. Since the dispersion of the particles is exponential during chaotic mixing, per Figure 9, a more detailed fit might have come from increasing the number of grid points for the chaotic part of the investigation. However, for this research effort it was decided that the sampling grid should be held constant.

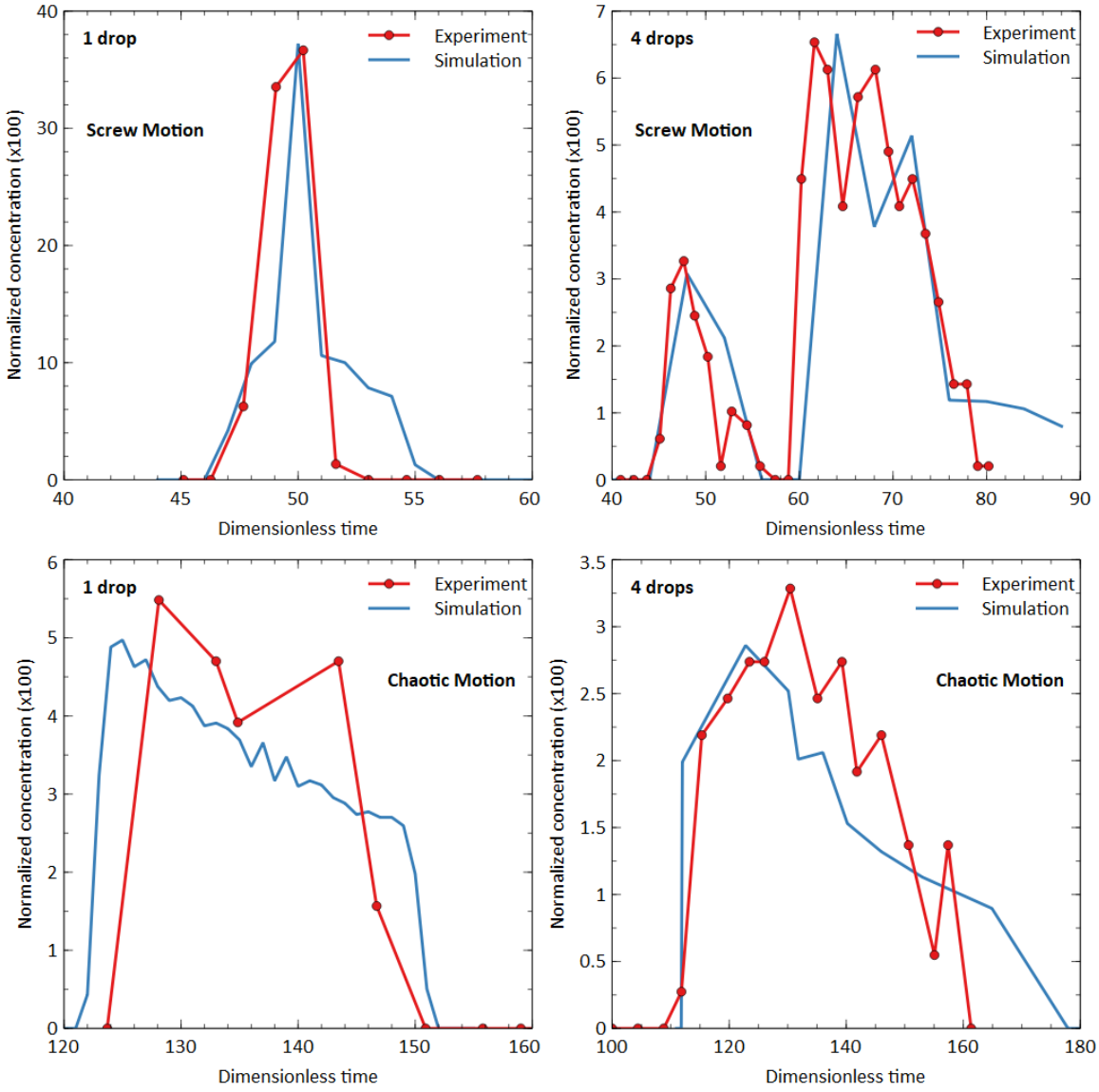

Figure 17. Comparison of the residence time distributions for screw and chaotic mixing for 1 drop (left) and for 4 drops (right[37,38]).

Conclusions

The biharmonic equation based analytical solution used in this work led to a computationally straightforward method for determining the three-dimensional flow field in the extruder channel. Chaotic mixing can be obtained in a free-helix extruder by the rotation of the helix and core at the same angular velocity, to emulate moving the barrel wall as one surface of the channel, and then rotating the screw core only, to emulate moving the opposite wall. When repeated in a periodic manner, deterministic chaotic motion results in the extruder screw channel. The experimental quantification of the model prediction of both the conventional extruder flow mixing and the chaotic mixing was facilitated by developing a new experimental technique that closely emulated a Dirac pulse or well-defined drops at the start of each experiment. The mixing experiments in this free-helix extruder demonstrated that substantially better mixing was obtained when the device was operated in the chaotic mode. This extrusion device when operated in the chaotic mode would provide better mixing for low concentration additives than conventional screw rotation. The chaotic mixing in the free-helix extruder reduces the effects of Moffatt eddies. The evaluation of the theoretical prediction from the code were consistent with literature demonstrations of exponential mixing for polymer processing systems operating in a way to induce chaotic flow.

References

[1] Rowell, H. S., Finlayson, D., "Screw Viscosity Pumps," *Engineering*. 1922;114: 606-608.

[2] Rowell, H. S., Finlayson, D., "Screw Viscosity Pumps," *Engineering*. 1928; 126: 249-250, 385-387.

[3] Tadmor, Z., Klein, I., *Engineering Principles of Plasticating Extrusion*. Krieger; 1978.

[4] Campbell, G. A., Spalding, M.A., *Analyzing and Troubleshooting Single-Screw Extruders*. Hanser Publishers; 2013.

[5] Tjahjadi, M., Foster, R. W., "US5551777: Single screw extruder capable of generating chaotic mixing," *General Electric Company*, (1995).

[6] Campbell, G. A., Bomma, S., St. John, S., et al., Residence time in a single screw free helix extruder using a new solution to the biharmonic equation. *Polym Eng Sci*. 2021;61(1):184-200. doi:10.1002/pen.25567

[7] Middleman, S., *Fundamentals of Polymer Processing*. McGraw-Hill; 1977.

[8] Chella, R., Ottino, J. M., "Fluid mechanics of mixing in a single-screw extruder," *Ind Eng Chem Fund*. 1985;24(2):170-180. doi:10.1021/i100018a006

[9] Campbell, G. A., Sweeney, P. A., Dontula, N., Wang, C., "Frame Indifference: Fluid Flow in Single Screw Pumps and Extruders," *Int. Polym. Proc*., 11, 199 – 207 (1996), DOI:10.3139/217.960199.

[10] Campbell, G. A., Wang, C., Cheng, H., Bullwinkel, M., te-Riele, M. A., "An Investigation of Flow Rate and Viscous Dissipation in the Single Screw Pump-Extruder," *International Polymer Processing*, XVI, 325, (2001).

[11] Malvern L. E., *Introduction to the Mechanics of a Continuous Medium*. Prentice-Hall; 1969.

[12] Polychronopoulos, N. D., Vlachopoulos, J., "Computer Flow Simulation of Moffatt Eddies," *Intern. Polymer Processing XXXIII* **5** 662 (2018).

[13] Jana S. C., Tjahjadi M., Ottino J. M., "Chaotic mixing of viscous fluids by periodic changes in geometry: Baffled cavity flow," *AIChE J*. 1994;40(11):1769-1781. doi:10.1002/aic.690401102

[14] Chien, W-L, Rising, H., Ottino, J. M., "Laminar mixing and chaotic mixing in several cavity flows," *J. Fluid Mech*. 1986; 170:355-377. doi:10.1017/S0022112086000927

[15] Hunt, D., *Determination of Flow Rates in Extrusion*. [Master's Thesis]. Potsdam, NY: Clarkson University. 1995.

[16] Wiggins S., Ottino, J. M., "Foundations of chaotic mixing," *Phil. Trans. R. Soc. Lond.A.* 2004 362, 937-970 doi: 10.1098/rsta.2003.1356

[17] Campbell, G. A., Sweeney, P. A., Dontula, N., Wang, C. H., "Frame Indifference: Fluid Flow in Single Screw Pumps and Extruders," *International Polymer Processing*. 1996;11(3):199-207. doi:10.3139/217.960199

[18] Joseph, D. D., Sturges L., "The Convergence of Biorthogonal Series for Biharmonic and Stokes Flow Edge Problems: Part II," *SIAM J Appl Math*. 1978;34(1):7-26. doi:10.1137/0134002

[19] Meleshko, V. V., "Steady Stokes flow in a rectangular cavity," *Proc R Soc Lond A*. 1996;452(1952):1999-2022. doi:10.1098/rspa.1996.0106

[20] Shankar, P. N., "The eddy structure in Stokes flow in a cavity," *J Fluid Mech*. 1993;250:371-383. doi:10.1017/S0022112093001491

[21] Chen, L., Lindt, J. T., "3-D flow effects on residence time distribution in screw extruders," *AIChE J*. 1996;42(6):1525-1535. doi:10.1002/aic.690420604

[22] Erwin, L., Mokhtarian, F., "Analysis of mixing in modified single screw extruders," *Polym Eng Sci*. 1983;23(2):49-60. doi:10.1002/pen.760230202

[23] Soulvaiotis, A., Jana, S. C., Ottino, J. M., "Potentialities and limitations of mixing simulations," *AIChE J*. 1995;41(7):1605-1621. doi:10.1002/aic.690410702

[24] Ling, F. H., Zhang, X., "Mixing of a Generalized Newtonian Fluid in a Cavity," *Journal of Fluids Engineering*. 1995;117(1):75-80. doi:10.1115/1.2816827

[25] Ling, F. H., "Chaotic mixing in the enhanced mixing simulator," *Polym Eng Sci*. 1995;35(11):929-941. doi:10.1002/pen.760351107

[26] Tjahjadi, M., Foster, R. W., inventors; General Electric Company, assignee. Single Screw Extruder Capable of Generating Chaotic Mixing. U.S. Patent No. 5,551,777. September 3, 1996:13.

[27] Aref, H., "Stirring by chaotic advection," *J. Fluid Mech*, 1984 **143**:1- 21.

[28] Anderson, P. D., Galaktionov, O. S., Peters, G. W. M., van de Vosse, F. N., Meijer, H. E.H., "Chaotic fluid mixing in non-quasi-static time-periodic cavity flows," *International Journal of Heat and Fluid Flow*. 2000;21(2):176-185. doi:10.1016/S0142-727X(99)00073-9

[29] Fountain, G. O., Khakhar, D. V., Mezić, I., Ottino, J. M., "Chaotic mixing in a bounded three-dimensional flow," *J Fluid Mech*. 2000;417:265-301. doi:10.1017/S002211200000118X

[30] Lamberto, D. J., Alvarez, M. M., Muzzino, F. J., "Computational Analysis of Regular and Chaotic Mixing in a Stirred Tank Reactor," *Chemical Engineering Science*, **56**, 4887 (2001).

[31] Kim, S. J., Kwon, T. H., "Enhancement of Mixing Performance of Single-Screw Extrusion Processes via Chaotic Flows: Part I. Basic Concepts and Experimental Study," *Advances in Polymer Technology*.

1996;15(1):41-54. doi:https://doi.org/10.1002/(SICI)1098-2329(199621)15:1<41::AID-ADV4>3.0.CO;2-K

[32] Kim, S. J., Kwon, T. H., "Enhancement of Mixing Performance of Single-Screw Extrusion Processes via Chaotic Flows: Part II. Numerical Study," *Advances in Polymer Technology*. 1996;15(1):55-69. doi:https://doi.org/10.1002/(SICI)1098-2329(199621)15:1<55::AID-ADV5>3.0.CO;2-J

[33] Xu, B., Liu, Y., Yu, H., Turng, L-S, "Chaotic mixing in a single-screw extruder with a moving internal baffle," *Polym Eng Sci*. 2014;54(1):198-207. doi:10.1002/pen.23531

[34] Zhu ,X., Tong, Y., Hu, Y., "Chaotic Manifold Analysis of Four-Screw Extruders Based on Lagrangian Coherent Structures," *Materials*. 2018;11(11):2272. doi:10.3390/ma11112272

[35] Liu, J., Zhu, X., "Chaotic mixing analysis of a novel single-screw extruder with a perturbation baffle by the finite-time Lyapunov exponent method," *Journal of Polymer Engineering*. 2019;39(3):287-299. doi:10.1515/polyeng-2018-0037

[36] Xu, B-P, He, L., Wang, M-G, Tan, S-Z, Yu, H-W, Turng, L-S, "Numerical Simulation of Chaotic Mixing in Single Screw Extruders with Different Baffle Heights," *International Polymer Processing*. 2016;31(1):108-118. doi:10.3139/217.3167

[37] Bomma, S., *Chaotic Mixing in Single Screw Extruders*. [Master's Thesis]. Potsdam, NY: Clarkson University. 2007.

[38] St. John, S., *Studying Chaotic Flow in a Single-Screw, Free-Helix Extruder Resulting from Time-Periodic Flow*. [Honors Thesis]. Potsdam, NY: Clarkson University. 2003.

[39] Chempath, S., *Flow Field in the Free-Helix Single-Screw Extruder*. [Master's Thesis]. Potsdam, NY: Clarkson University. 1999.

[40] Galaktionov, O. S., Anderson, P. D., Peters, G. W. M., Meijer, H. E. H., "Mapping approach for 3D laminar mixing simulations: application to industrial flows," *Numerical Methods in Fluids*. 2002; 40(3-4): 345-351.

[41] Bur, A., "Fluorescence Monitoring of Twin Screw Extrusion," *Polymer Engineering and Science.* 1991;31(18):1366-1370.